

5-2000

# Crystal and Magnetic Structures of $\text{LaNi}_5-x\text{Mnx}$

C. Y. Tai

*University of Missouri - Rolla*

G. K. Marasinghe

*University of Missouri - Rolla*

O. A. Pringle

*University of Missouri - Rolla*

W. J. James

*University of Missouri - Rolla*

M. Chen

*University of Missouri - Columbia*

*See next page for additional authors*

Follow this and additional works at: [http://opensiuc.lib.siu.edu/phys\\_pubs](http://opensiuc.lib.siu.edu/phys_pubs)

© 2000 American Institute of Physics

Published in *Journal of Applied Physics*, Vol. 87 No. 9 (2000) at doi: [10.1063/1.372823](https://doi.org/10.1063/1.372823)

## Recommended Citation

Tai, C. Y.; Marasinghe, G. K.; Pringle, O. A.; James, W. J.; Chen, M.; Yelon, W. B.; Dubenko, I.; Ali, N.; and l'Héritier, Ph., "Crystal and Magnetic Structures of  $\text{LaNi}_5-x\text{Mnx}$ " (2000). *Publications*. Paper 46.

[http://opensiuc.lib.siu.edu/phys\\_pubs/46](http://opensiuc.lib.siu.edu/phys_pubs/46)

---

**Authors**

C. Y. Tai, G. K. Marasinghe, O. A. Pringle, W. J. James, M. Chen, W. B. Yelon, I. Dubenko, N. Ali, and Ph. l'Héritier

# Crystal and magnetic structures of $\text{LaNi}_{5-x}\text{Mn}_x$

C. Y. Tai, G. K. Marasinghe, O. A. Pringle, and W. J. James

*Department of Physics, Department of Chemistry, and The Graduate Center for Materials Research, University of Missouri–Rolla, Rolla, Missouri 65409*

M. Chen and W. B. Yelon

*Research Reactor, University of Missouri–Columbia, Columbia, Missouri 65211*

I. Dubenko and N. Ali

*Department of Physics, Southern Illinois University at Carbondale, Carbondale, Illinois 62901*

Ph. l'Héritier

*Laboratoire des Matériaux et du Genie Physique, ENS de Physique de Grenoble, France*

The crystallographic and magnetic properties of  $\text{LaNi}_{5-x}\text{Mn}_x$  with  $x=1, 1.5,$  and  $2,$  have been investigated using x-ray and neutron diffraction, vibrating sample magnetometer and superconducting quantum interference device measurements. All the samples crystallize in the hexagonal  $\text{CaCu}_5$ -type ( $P6/mmm$ ) structure. Manganese atoms preferentially occupy the  $3g$  site in the  $\text{LaNi}_5$  structure. The bulk magnetization of the  $\text{LaNi}_{5-x}\text{Mn}_x$  powder samples decreases rapidly as nickel is replaced by manganese. A ferrimagnetic model is applied to describe the magnetic structure of the  $\text{LaNi}_{5-x}\text{Mn}_x$  samples for  $x=1.5$  and  $2.$  A ferromagnetic model gives the best fit of the neutron diffraction data for the  $\text{LaNi}_4\text{Mn}$  sample. © 2000 American Institute of Physics. [S0021-8979(00)77408-1]

## I. INTRODUCTION

Even though rare earth–transition-metal (R–M) intermetallics are the leading candidates for the next-generation permanent magnets, the relationship between the electronic structure and the magnetic properties of these compounds has not been fully understood. An explanation based on electronic structure as to why negative magnetic interactions are more common in R–Mn intermetallics than in R–Fe intermetallics<sup>1</sup> will be helpful in engineering the next generation of commercial permanent magnets. We intend to make use of recent developments<sup>2</sup> in spin-resolved photoemission spectroscopy to study in detail the band structure of these intermetallics. Because the interpretation of spin-resolved photoemission spectra of complex intermetallics such as  $\text{RM}_{12}$  and  $\text{R}_2\text{M}_{17}$  is very difficult, it is prudent to start with the relatively simple  $\text{RM}_5$  system. However, because  $\text{RFe}_5$  and  $\text{RMn}_5$  intermetallics do not exist, we will study the electronic structures of the  $\text{LaNi}_{5-x}\text{Fe}_x$  and  $\text{LaNi}_{5-x}\text{Mn}_x$  systems.

A good understanding of the crystallographic and magnetic properties of these intermetallics is necessary to accurately interpret their spin-resolved photoemission spectra. The  $\text{LaNi}_{5-x}\text{Fe}_x$  system has been investigated in detail in previous studies.<sup>3–5</sup> These studies suggested the coexistence of long-range ferromagnetic ordering and spin-glass-like localized clusters. The crystallographic properties of  $\text{LaNi}_{5-x}\text{Mn}_x$  at 295 K have also been studied<sup>6,7</sup> using x-ray and neutron diffraction. In the present study, the magnetic structures and properties of  $\text{LaNi}_{5-x}\text{Mn}_x$  are investigated using low-temperature neutron diffraction, superconducting quantum interference device (SQUID), and vibrating sample magnetometer (VSM) measurements, and are compared with those properties of  $\text{LaNi}_{5-x}\text{Fe}_x$ .<sup>3</sup>

## II. EXPERIMENT

The  $\text{LaNi}_{5-x}\text{Mn}_x$  samples were prepared from elements of 99.99% purity or higher by induction melting in a cold copper crucible. Induction-melted ingots were annealed for two weeks at 750 °C. The phase purity of the samples was checked by x-ray diffraction with  $\text{Cu } K\alpha$  radiation on a Scintag XDS 2000 x-ray diffractometer equipped with a single-crystal graphite monochromator. The powder neutron diffraction data were obtained at the University of Missouri Research Reactor using neutrons of wavelength 1.4875 Å. The samples were placed in thin-walled vanadium containers, and neutron diffraction data were collected at 20 and 295 K for 4–6 h. The diffraction data were refined by the Rietveld technique.<sup>8</sup> The bulk magnetic properties of the powder samples were measured at Southern Illinois University–Carbondale on a Quantum Design SQUID magnetometer, and at the Laboratoire des Matériaux et du Genie Physique (LMGP) in France on an Oxford VSM or Foner-type magnetometer.

## III. RESULTS AND DISCUSSIONS

The  $\text{LaNi}_{5-x}\text{Mn}_x$  samples crystallized in the  $\text{CaCu}_5$ -type structure (space-group  $P6/mmm$ ) with little (<5 at. %) or no impurities. Table I gives the lattice parameters and site occupancies of  $\text{LaNi}_{5-x}\text{Mn}_x$  compounds obtained from Rietveld refinements of the neutron diffraction data, and Fig. 1 shows the neutron diffraction data and fit for  $\text{LaNi}_{3.5}\text{Mn}_{1.5}$  at 20 K. The weak peak at  $2\theta \approx 23^\circ$  is due to a nonmagnetic impurity. The unit cell expands with increasing manganese content at a rate of  $\sim 5.5\%$  per substituted atom. This expansion rate is more than twice the rate of 2.5% per substituted atom observed in  $\text{LaNi}_{5-x}\text{Fe}_x$ ,<sup>3</sup> which also crystallized in the  $\text{CaCu}_5$ -type structure. The difference in expansion rates

TABLE I. Lattice parameters, unit-cell volumes, and manganese site occupancies for  $\text{LaNi}_{5-x}\text{Mn}_x$ .

	295 K			20 K			% Mn occ.	
	$a$ (Å)	$c$ (Å)	$V$ (Å <sup>3</sup> )	$a$ (Å)	$c$ (Å)	$V$ (Å <sup>3</sup> )	3g	2c
$\text{LaNi}_5$	5.0162(1)	3.9837(1)	86.812(3)	...	...	...	...	...
$\text{LaNi}_4\text{Mn}$	5.0940(2)	4.0697(2)	91.456(7)	5.0690(2)	4.0527(2)	90.182(7)	29.4(3)	5.2(5)
$\text{LaNi}_{3.5}\text{Mn}_{1.5}$	5.1392(2)	4.1104(2)	94.017(7)	5.1147(1)	4.0966(1)	92.810(3)	45.1(3)	6.1(6)
$\text{LaNi}_3\text{Mn}_2$	5.1941(2)	4.1408(2)	96.746(7)	5.1741(2)	4.1329(2)	95.819(7)	60.8(3)	7(1)

is most likely due to the size difference between iron and manganese atoms ( $r_{\text{Fe}} = 1.27 \text{ \AA}$  and  $r_{\text{Mn}} = 1.31 \text{ \AA}$ ). The substitutional occupancy patterns in the two series of samples, however, are similar. As was the case for iron in  $\text{LaNi}_{5-x}\text{Fe}_x$ , manganese atoms in the  $\text{LaNi}_{5-x}\text{Mn}_x$  samples preferentially substitute for nickel atoms at the 3g site.

A comparison of the neutron diffraction patterns measured at 20 and 295 K, see Fig. 2, illustrates the effects of the magnetic structure on neutron scattering in  $\text{LaNi}_{5-x}\text{Mn}_x$ . The large intensities of the (100) and (101) reflections in the diffraction patterns measured at 20 K are due to magnetic

scattering. Furthermore, the difference between the intensities of these peaks at 20 and 295 K suggests that the atoms responsible for the observed magnetic scattering, predominantly the manganese atoms, possess appreciable magnetic moments.

Figure 3, which compares the magnetization versus temperature ( $M$  vs  $T$ ) data for  $\text{LaNi}_{5-x}\text{Fe}_x$  and  $\text{LaNi}_{5-x}\text{Mn}_x$ , illustrates the different effects of partially substituting the nickel sublattice with iron or manganese in  $\text{LaNi}_5$ . As seen in Fig. 3(a), partial substitution for nickel by iron increases the net magnetization of  $\text{LaNi}_5$ . Furthermore, the magnetic behavior of  $\text{LaNi}_{5-x}\text{Fe}_x$  samples with  $x \geq 1.2$  is indicative of ferromagnetic ordering.<sup>9</sup> In contrast, the net magnetization of  $\text{LaNi}_{5-x}\text{Mn}_x$  intermetallics decreases with increasing manganese content. The shapes of the  $M$  vs  $T$  curves and the weak magnetization values ( $< 0.7 \text{ emu/g}$ ) for  $\text{LaNi}_{5-x}\text{Mn}_x$  intermetallics are not those of typical ferromagnetically ordered materials. In addition, these intermetallics do not reach magnetic saturation even at applied fields as high as 15 T.<sup>10</sup> These observations, when combined with the fact that manganese atoms possess non-negligible magnetic moments, point to a magnetic structure consisting of a ferrimagnetically ordered manganese sublattice. As described below, detailed analysis of neutron diffraction data measured at 20 K confirms the existence of such a magnetic structure in the  $\text{LaNi}_{5-x}\text{Mn}_x$  intermetallics.

To simplify the analysis of the magnetic scattering contribution to the neutron diffraction data, the magnetic moments on the 2c manganese atoms were neglected due to the very small manganese occupancy of that site. Based on this assumption, the manganese atoms at the 3g sites are mainly responsible for the magnetic effects. Because all the magnetic reflections are allowed reflections of the  $P6/mmm$  space group, the crystallographic and magnetic unit cells are the same. Due to the observed weak magnetization values and the strong magnetic reflections, refinements of the 20 K neutron diffraction data of the  $\text{LaNi}_{5-x}\text{Mn}_x$  samples with  $x = 1.5$  and 2.0 were done with a ferrimagnetic model. In this model, the three crystallographically identical 3g sites occupied by the manganese atoms, labeled 3g-1, 3g-2, and 3g-3 in Fig. 4, are magnetically nonequivalent. The best fits of the neutron diffraction pattern were obtained when it is assumed that the magnetic moment of the manganese atom at the 3g-1 site is antiparallel to those at the 3g-2 and 3g-3 sites. This magnetic structure can be considered as a stacking of ferromagnetic sheets, where the magnetic moments are aligned parallel within each vertical sheet but alternate in direction in adjacent layers. In order to obtain better fits,

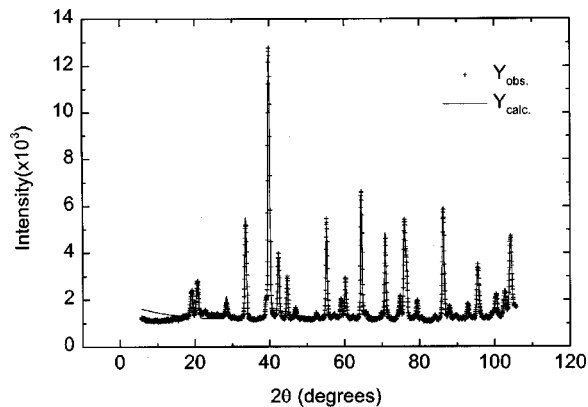


FIG. 1. Neutron diffraction pattern measured at 20 K for  $\text{LaNi}_{3.5}\text{Mn}_{1.5}$  and fit based on the  $\text{CaCu}_5$ -type structure and the ferrimagnetic mode.

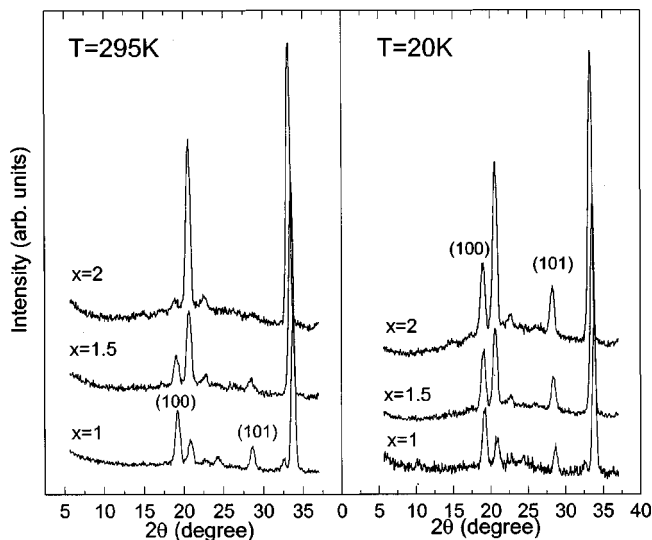


FIG. 2. Neutron diffraction patterns at 295 and 20 K for the  $\text{LaNi}_{5-x}\text{Mn}_x$  samples. All peaks are normalized to the 111 reflections, which are not shown in the patterns.

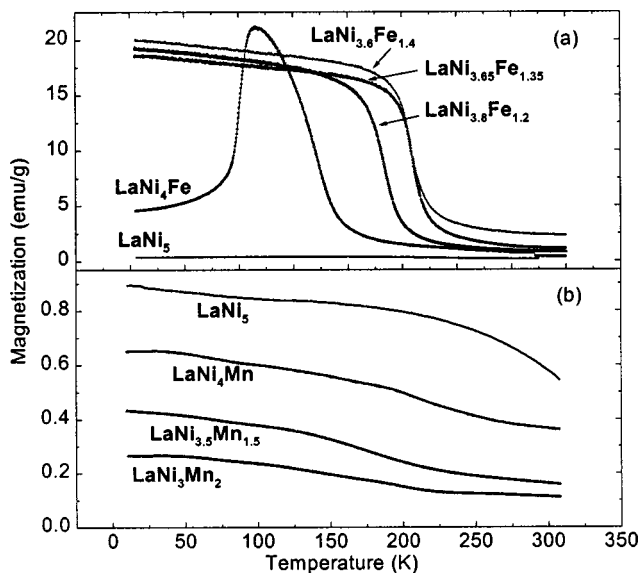


FIG. 3. Magnetization vs temperature for (a)  $\text{LaNi}_{3-x}\text{Fe}_x$  ( $H=1000$  Oe) and (b)  $\text{LaNi}_{5-x}\text{Mn}_x$  ( $H=2000$  Oe).

weak moments ( $0.1 \mu_B$  or less) on the  $2c$  and  $3g$  nickel atoms were included in the refinements. The nickel moments, which might be induced by the manganese moments, are parallel to the net magnetic moment of the manganese sublattice. These weak moments could also be an artifact resulting from the neglected manganese moments at the  $2c$  site, although they are similar to the induced moments found in  $\text{LaNi}_{5-x}\text{Fe}_x$ .<sup>3,4</sup> The fit shown in Fig. 1 was obtained using this ferrimagnetic model.

For the  $\text{LaNi}_4\text{Mn}$  sample, however, a ferromagnetic model in which the magnetic moments of all manganese atoms are parallel gives the best fit of the neutron diffraction pattern at 20 K. Probability calculations show that the

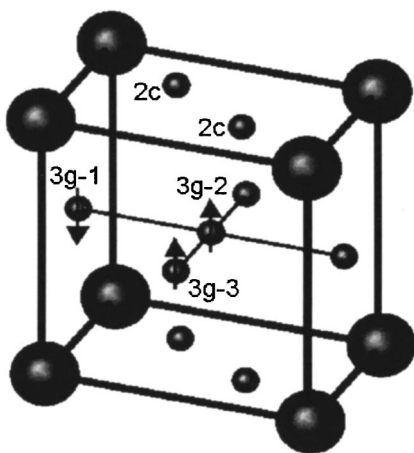


FIG. 4.  $\text{LaNi}_{5-x}\text{Mn}_x$  structure showing the antiparallel coupling of the manganese  $3g$  moments. The larger atoms are La and the smaller ones are either Ni or Mn.

TABLE II. Total magnetic moments for  $\text{LaNi}_{5-x}\text{Mn}_x$ .

	$\mu_{\text{total}}$ ( $\mu_B/\text{f.u.}$ )	$\theta^a$ (degrees)
$\text{LaNi}_4\text{Mn}$	1.59	0
$\text{LaNi}_{3.5}\text{Mn}_{1.5}$	1.11	90
$\text{LaNi}_3\text{Mn}_2$	1.07	115

<sup>a</sup>Angle between the  $z$  axis and moment direction.

$\text{LaNi}_4\text{Mn}$  compound has only 0.68 Mn–Mn nearest-neighbor pairs at the  $3g$  site per unit cell. It means that the chance of having negative exchange (Mn–Mn antiparallel coupling) at the  $3g$  site is less than 23% ( $0.68:3 \approx 0.226:1$ , where 3 is the maximum possible number of nearest-neighbor pairs at the  $3g$  site), which explains the ferromagnetic behavior of the  $\text{LaNi}_4\text{Mn}$  sample due to the dilute manganese concentration. The magnetic moments of the  $3g$  manganese atoms obtained from the refinements are 1.25, 1.50, and  $1.20 \mu_B$  for the  $x = 1, 1.5$ , and 2 samples. Table II gives the magnitude and direction of the total magnetic moments calculated from the neutron data refinements. The refined results suggest the rotation of the total moment direction away from the  $z$  axis to the  $xz$  plane when the manganese content increases. The total moment decreases with manganese content in agreement with the  $M$  vs  $T$  data [Fig. 3(b)].

### ACKNOWLEDGMENTS

The authors acknowledge the financial support of the National Science Foundation for Grant No. DMR-9614596 and the Defense Advanced Research Projects Agency for Grant No. DAAG 55-98-1-0267. The work conducted at the Southern Illinois University–Carbondale (SIUC) was supported by the Materials Technology Center–SIUC.

- <sup>1</sup>W. E. Wallace, *Rare Earth Intermetallics* (Academic, New York, 1973), pp. 181, 184, and 188.
- <sup>2</sup>J. P. Woods, B. M. Patterson, A. S. Fernando, and S. S. Jaswal, *Phys. Rev. B* **51**, 1064 (1995).
- <sup>3</sup>C. Y. Tai, C. Tan, G. K. Marasinghe, O. A. Pringle, W. J. James, M. Chen, W. B. Yelon, J. Gebhardt, and N. Ali, *IEEE Trans. Magn.* **35**, 3346 (1999).
- <sup>4</sup>J. Lamloumi, A. Percheron-Guégan, J. C. Achard, G. Jehanno, and D. Givord, *J. Phys. (France)* **45**, 1643 (1984).
- <sup>5</sup>M. Escorne, J. Lamloumi, A. Percheron-Guégan, J. C. Achard, A. Mauger, and G. Jehanno, *J. Appl. Phys.* **63**, 4121 (1988).
- <sup>6</sup>C. Lartigue, A. Percheron-Guégan, J. C. Achard, and F. Tassett, in *Rare Earths in Modern Science and Technology*, edited by G. J. McCarthy, J. J. Rhyne, and H. B. Silber (Plenum, New York, 1980), Vol. 2, p. 585.
- <sup>7</sup>A. Percheron-Guégan, J. C. Achard, P. Germi, and F. Tassett, *J. Less-Common Met.* **74**, 1 (1980).
- <sup>8</sup>J. Rodriguez-Carvajal, computer code FULLPROF version 3.0.0 (Laboratoire Leon Brillouin, France, 1995).
- <sup>9</sup>B. D. Cullity, *Introduction to Magnetic Materials* (Addison-Wesley, Reading, MA, 1972), p. 203.
- <sup>10</sup>C. Lartigue, A. Percheron-Guégan, K. A. Gschneidner, Jr., *J. Less-Common Met.* **88**, 211 (1982).